

# Detecting and Tuning the Interactions between Surfactants and Carbon Nanotubes for Their High-Efficiency Structure Separation

Xiang Zeng, Dehua Yang, Huaping Liu,\* Naigen Zhou, Yanchun Wang, Weiya Zhou, Sishen Xie, and Hiromichi Kataura\*

The selective interaction is systematically explored between the surfactants (sodium deoxycholate (DOC), sodium dodecyl sulfate (SDS), and sodium cholate (SC)) and the single-wall carbon nanotubes (SWCNTs) by the gel chromatography technique. The results show that DOC preferentially interacts with small-diameter semiconducting SWCNTs (S-SWCNTs), exhibiting the strongest interaction strength for the SWCNTs, and the highest structural selectivity. The surfactant SC shows high selectivity toward the chiral angles of the SWCNTs. Its interaction strength and structural recognition ability are slightly higher than that of SDS but lower than that of DOC. Combining with the proved selectivity of SDS in the adsorption onto the S-SWCNTs with small C–C bond curvature, it is discovered that the synergistic effect of the triple surfactants amplified the interaction difference among the different SWCNTs and the gel, and thus dramatically improved the separation efficiency and structural purity of the SWCNTs, achieving the separation of distinct ( $n, m$ ) single-chirality species and their enantiomers in one step. This work not only provides deeper insights into the separation mechanism of SWCNTs with the surfactant sorting techniques, but also has a profound significance in studying the interaction between the SWCNTs and other small molecules.

in electronics, optics, and other related areas.<sup>[1–9]</sup> However, the current synthetic methods of SWCNTs difficultly produce a population of single-structure SWCNTs with identical properties despite recent creative breakthroughs in controlling the structural growth,<sup>[10–13]</sup> which seriously restricts the evaluation of their property and the corresponding technical applications. The structural control of SWCNTs by the postgrowth separation methods are more developed. Until now, various separation techniques such as DNA wrapping chromatography,<sup>[14,15]</sup> polymer wrapping,<sup>[16,17]</sup> density gradient ultracentrifugation (DGU),<sup>[18,19]</sup> aqueous two-phase extraction (ATPE),<sup>[20–22]</sup> and gel chromatography<sup>[23,24]</sup> have been developed for the structural sorting of the synthetic SWCNT mixtures. With these techniques, SWCNTs can be separated based on not only their electronic type (i.e., metallic and semiconducting SWCNTs) but also chirality. In these solution-sorting techniques,

the selective interactions of DNA, polymers, or surfactants with the SWCNTs is critical for their separation efficiency and purity. DGU, ATPE, and gel chromatography are currently the major methods because of the possibility of the mass production of single-chirality SWCNTs.<sup>[18–24]</sup> The principal feature in these methods is that the surfactants like sodium dodecyl sulfate

## 1. Introduction

The optical and electronic properties of single-wall carbon nanotubes (SWCNTs) are solely determined by their diameters and chiral angles. Thus, structural control of SWCNTs is critical for their basic research and technical applications

X. Zeng, Dr. D. H. Yang, Prof. H. P. Liu, Dr. Y. C. Wang,  
Prof. W. Y. Zhou, Prof. S. S. Xie  
Beijing National Laboratory for Condensed Matter Physics  
Institute of Physics  
Chinese Academy of Sciences  
Beijing 100190, China  
E-mail: liuhuaping@iphy.ac.cn

X. Zeng, Dr. D. H. Yang, Prof. H. P. Liu, Dr. Y. C. Wang,  
Prof. W. Y. Zhou, Prof. S. S. Xie  
Beijing Key Laboratory for Advanced Functional  
Materials and Structure Research  
Beijing 100190, China

 The ORCID identification number(s) for the author(s) of this article can be found under <https://doi.org/10.1002/admi.201700727>.

DOI: 10.1002/admi.201700727

X. Zeng, Prof. N. G. Zhou  
School of Materials Science and Engineering  
Nanchang University  
Nanchang, 30031, China

Dr. D. H. Yang, Prof. H. P. Liu, Prof. W. Y. Zhou, Prof. S. S. Xie  
School of Physical Sciences  
University of Chinese Academy of Sciences  
Beijing 100049, China

Prof. H. P. Liu, Prof. S. S. Xie  
Collaborative Innovation Center of Quantum Matter  
Beijing 100190, China

Prof. H. Kataura  
Nanomaterials Research Institute  
National Institute of Advanced Industrial Science and Technology (AIST)  
Tsukuba, Ibaraki 305-8565, Japan  
E-mail: h-kataura@aist.go.jp

(SDS), sodium cholate (SC), and by sodium deoxycholate (DOC) are used to tune the density (DGU), surface wettability (ATPE), or the surface charge density of the distinct  $(n, m)$  SWCNTs (gel chromatography) for their structural separation.<sup>[19–30]</sup> However, the lack of understanding of the selective interaction between the surfactants and the SWCNTs limits the separation efficiency, purity, and the types of the SWCNT species.

Here, we systematically investigated the selective interaction of the surfactants with different chiral SWCNTs by the gel chromatography technique. Compared with the ATPE and DGU techniques, the gel chromatography does not need expensive density gradient agents or other chemical agents, and is a simple and efficient way to investigate the selective interaction between the surfactants and the SWCNTs.<sup>[23–26]</sup> In a typical gel-based method, SWCNTs are dispersed in water with one of the surfactants (SDS, DOC, and SC) or their mixture. These surfactant-wrapped SWCNTs with different structures can be separated on the basis of their interaction difference with an allyl dextran-based gel, which results from the difference in the coverage and/or thickness of the surfactant coating around the different  $(n, m)$  species due to the selective interaction between the surfactants and the SWCNTs.<sup>[23–26,30–33]</sup> A higher coverage or a thicker surfactant coating having a high density of negative charges on the SWCNT surfaces would lead to their strong repulsion from the surfactant-functionalized gel, and thus, to weaker adsorbability,<sup>[31,32]</sup> (as shown in **Figure 1**). Therefore, the selective interaction between the surfactants and the SWCNTs can be easily judged by the adsorption or the desorption processes of the distinct  $(n, m)$  SWCNTs onto/from the gel. Although our group and other researchers recently reported the selective interactions of these surfactants with SWCNTs by similar methods,<sup>[30,32,34]</sup> a more systematical and refined investigation is lacking, which could not give a complete image of the selective interaction between the surfactants and the nanotubes.

In this work, the selective interaction of DOC and SC molecules with SWCNTs was investigated by varying their

concentrations to explore the adsorbability/desorbability of the SWCNTs onto/from the gel. Since previous works showed that SDS is an essential and indispensable ingredient in the gel-based separation of SWCNTs,<sup>[35]</sup> the separation experiments herein were conducted in the presence of SDS. Specifically, the SDS-dispersed SWCNT solution was loaded into gel columns, and the adsorbed SWCNTs were eluted by varying the DOC, SDS, or SC concentrations in the eluents (**Figure S1**, Supporting Information). Thus, their selective interactions with the different-structure SWCNTs could be determined from the elution order of the adsorbed SWCNTs. The results show that the surfactants DOC and SC preferentially interact with the SWCNTs by diameter and chiral angle, respectively. DOC exhibited the strongest interaction strength and the highest structural recognition ability for the SWCNTs. By contrast, SDS showed the weakest interaction strength and the lowest structural recognition ability for the SWCNTs, which explained that the SDS-encapsulated SWCNTs more easily adsorbed onto gel. Combining with the previously demonstrated selectivity of SDS toward the smallest C–C bonds of the SWCNTs, we discovered that the synergic effect of the three surfactants increased the interaction difference between the different SWCNT structures and the gel, thereby facilitating high-efficiency separation of distinct  $(n, m)$  species and their enantiomers.

## 2. Results and Discussion

The selective interaction between the surfactants and the SWCNTs was investigated as follows (**Figure S1**, Supporting Information): (i) The as-prepared SWCNT dispersions were overloaded into the gel columns, which ensured that the adsorbed nanotubes would have a narrower structural distribution. (ii) The adsorbed nanotubes were eluted by incrementally increasing the concentration of one surfactant. During the step-wise elution, the eluents were 1 wt% SDS +  $x$  wt% A, in which

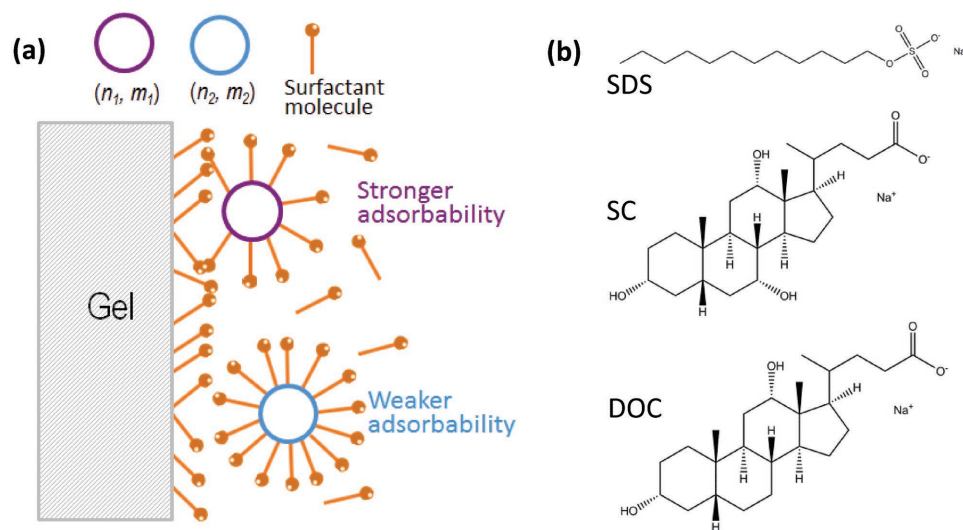


**Figure 1.** a) The diagram for the surfactants tuning the interaction between the SWCNTs and the gel. A higher density surfactant coating would lead to a weaker adsorbability of an SWCNT to gel. The purple and blue circles respectively represent different-structure SWCNTs, which are indicated by indexes of  $(n_1, m_1)$  and  $(n_2, m_2)$ . Brown bars denote surfactant molecules. b) The chemical structures of the surfactants sodium dodecyl sulfate (SDS), sodium cholate (SC), and sodium deoxycholate (DOC).

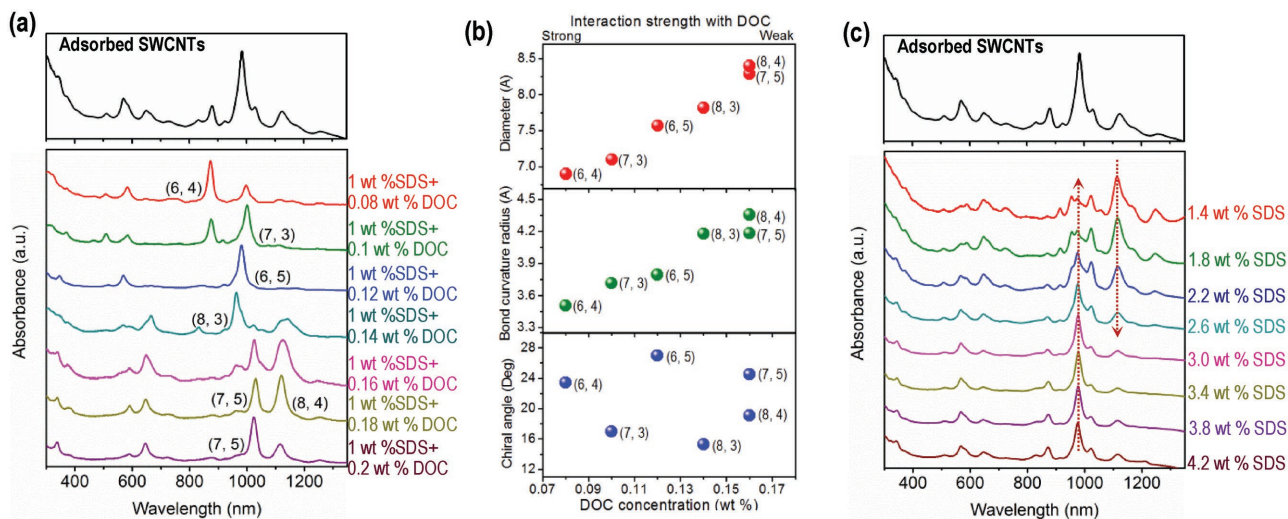


**Figure 2.** Optical analysis of the eluted fractions with increased DOC and SDS concentrations. a) Normalized optical absorption spectra of the eluted SWCNT fractions at increasing DOC concentrations. b) The elution order of distinct  $(n, m)$  species as a function of their diameters (top of panel), smallest bond curvature radius (middle of panel) and chiral angles (bottom of panel) at increasing the DOC concentrations. c) Normalized optical absorption spectra of the eluted SWCNT fractions at increasing SDS concentrations.

A can be SDS, DOC, or SC and  $x$  is the variable concentration of A with a stepwise increase. (iii) The elution order of the various  $(n, m)$  SWCNTs and their selective interaction with the surfactants were analyzed. The early-eluted SWCNTs exhibited a stronger interaction with the corresponding surfactants due to a higher coverage or a thicker coating on their surfaces, thus suppressing the interaction with the gel.

### 2.1. Selective Interaction of DOC with SWCNTs

As mentioned above, the experiment consisted of two steps: overloading and the stepwise elution process. Initially, a 10 mL aliquot of SDS/SWCNT dispersion was applied to a column packed with 1.4 mL of gel beads under 1 wt% SDS followed by the removal of the unadsorbed nanotubes. The totally adsorbed nanotubes in the column were eluted by one step with an aqueous solution of 0.5 wt% DOC. The optical absorption spectrum is presented in the top panel of Figure 2a, which shows that the adsorbed SWCNTs are highly enriched in (6, 5) SWCNTs with a narrow diameter distribution, indicating the successful extraction of these nanotubes from the initial SWCNT mixture via the overloading process. Next, the adsorbed nanotubes were eluted using a mixture of SDS and DOC eluents in which the DOC concentration was increased from 0.02 to 0.2 wt% in increments of 0.02 wt%, while the SDS concentration was fixed at 1 wt%. As shown in the lower panels of Figure 2a and Figure S2a (Supporting Information), the distinct absorption spectra of the eluted fractions show that the adsorbed SWCNTs were selectively desorbed, and their chiral structures were separated.

Five distinct species were collected at different DOC concentrations; especially, near single-chiral (6, 4), (6, 5), and (7, 5) nanotubes were obtained, which could give a clear elution order of distinct  $(n, m)$  species. As shown in Figure 2b, the elution order more strongly depends on the SWCNT diameters.<sup>[36]</sup>

The smaller-diameter species desorbed first, followed by the large-diameter SWCNTs with increasing DOC concentration.<sup>[37]</sup> Since the only variable was the DOC concentration in the eluents, the difference in the surfactant density resulted from the selective interaction of DOC with different-structure SWCNTs. Clearly, DOC is more inclined to encapsulate the small-diameter nanotubes.

For a comparison with DOC, a parallel experiment was performed in which the adsorbed nanotubes were eluted by a stepwise increase in the SDS concentration (as shown in Figure 2c; Figure S2b, Supporting Information). The SDS concentration was increased in increments of 0.4 wt%. A smaller increment could not desorb the nanotubes. At 1.4 wt% SDS, a mixture of SWCNTs was eluted in which a high content of large-diameter SWCNTs were present compared to that in the adsorbed nanotubes. With increasing the SDS concentrations, the large-diameter SWCNTs in the eluted fractions decreased, and consequently, the eluted fractions were enriched in (6, 5) SWCNTs. The results indicate that the SDS molecules preferentially adsorbed onto the large-diameter nanotubes, which is consistent with our previous works.<sup>[24]</sup> More accurately, the selective interaction of SDS more strongly depended on the smallest C–C bond curvature radius (Figure S2c of ref. [24]). Only one type of near single-chirality (6, 5) SWCNTs was separated, which indicated that SDS has a lower chiral selectivity than does DOC. By contrast, the separation of high-purity  $(n, m)$  species by a much smaller increment of DOC concentration proved that DOC had a stronger interaction with the SWCNTs than did SDS. The difference in the elution ability might be derived from the fact that the planar DOC molecule has a much stronger affinity with the SWCNTs than does the linear SDS and forms a much more homogeneous micellar structure around the SWCNTs (as shown in Figure 1b).<sup>[38,39]</sup>

As shown in Figure 3a and Figure S2a (Supporting Information), the nonselective mass desorption of the adsorbed SWCNTs occurred when the initial concentration of DOC was

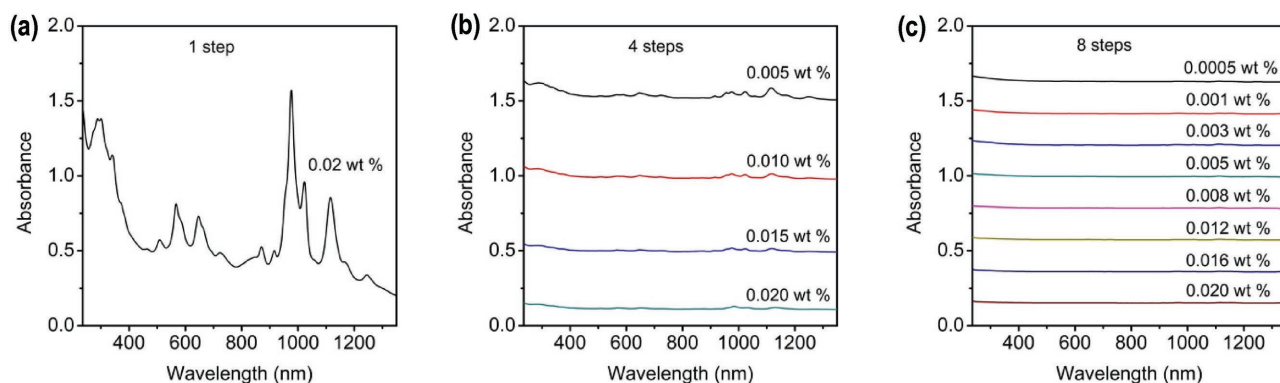


**Figure 3.** Optical absorption spectra of nonselectively desorbed SWCNTs under different starting concentrations and incremental steps of DOC. a) Starting concentration 0.02 wt%, and a step to 0.02 wt%. b) Starting concentration 0.005 wt% and four steps to 0.02 wt%. c) Starting concentration 0.0005 wt% and eight steps to 0.02 wt%.

set at 0.02 wt% in the first elution step, which led to a dramatic decrease in the yield of the following eluted SWCNTs. During the subsequent elution steps, nonselective mass desorption was not observed. A similar observation was made when the flow-through fraction was repeatedly loaded into the following columns (Column 2–Column 4) (as shown in Figure S3, Supporting Information). Interestingly, when the starting concentration of DOC and the increment step was decreased to 0.005 wt%, the nonselective desorption of SWCNTs reduced dramatically (Figure 3b; Figure S4a, Supporting Information); with a further decrease in the starting concentration and the increment step, the nonselective mass desorption of SWCNTs was not observed (Figure 3c; Figure S4b, Supporting Information). The nonselective DOC encapsulation of the SWCNTs under a high starting concentration might be attributed to the huge difference in its affinity/or interaction with the SWCNTs as compared to that of the SDS.<sup>[30,35]</sup> The introduction of a high-concentration DOC solution resulted in a high DOC concentration gradient and abruptly destroyed the equilibrium adsorption state of the nanotubes onto gel in the pure SDS system. On the other hand, although a lower DOC concentration gradient could avoid the nonselective mass desorption, the structural purity of the eluted SWCNTs clearly decreased (Figure S4b,c, Supporting Information). These results indicate that the separation of SWCNTs is greatly affected by the DOC concentration gradient.

## 2.2. Selective Interaction between the SC Molecules and the SWCNTs

The selective interaction between the SC molecules and the SWCNTs was investigated by eluting the adsorbed nanotubes with increasing SC concentration from 0.01 to 1.6 wt%, while the SDS concentration was fixed at 1 wt%. Figure 4a; Figure S5 (Supporting Information) present the optical absorption spectra of the eluted fractions. The eluted SWCNT fractions exhibited a lower structural purity than those eluted with DOC, with some fractions having specific species enrichment such as (8, 3) and (7, 3) SWCNTs in the case of 1 wt% SDS + 1.2 wt% SC and 1 wt% SDS + 1.6 wt% SC. Such concentrated desorption

of the species in a certain elution step could not be realized in the monosurfactant system of achiral SDS in which they gradually desorbed from the gel at each step. The changes in their absorption spectra (as shown in Figure 4 and Figure S5, Supporting Information) confirmed a rough desorption order for the different  $(n, m)$  species: (6, 5) – (7, 5) – (7, 6), (8, 4) – (8, 3) – (7, 3), (9, 1). The relationship between the elution order and the corresponding physical structures including diameters, the smallest C–C bond curvature radius and chiral angles are summarized in Figure 4b. Clearly, the elution order exhibits a strongest dependence on the chiral angles of the SWCNTs. Specifically, the early-eluted nanotubes had larger chiral angles and the late-eluted SWCNTs had smaller chiral angles, which implied that SC preferentially interacted with SWCNTs having larger chiral angles; this observation was different from that of SDS and DOC.

In order to further confirm the strong dependence of the selective interaction of SC with the SWCNTs on the chiral angles, the selective adsorption of the SWCNTs onto the gel under different ratios of SC to SDS was investigated by the overloading method. Four ratios of SC to SDS, namely, 1 wt% SDS + 0 wt% SC, 0.8 wt% SDS + 0.2 wt% SC, 0.5 wt% SDS + 0.5 wt% SC, 0.2 wt% SDS + 0.8 wt% SC, were respectively used to disperse and separate the SWCNTs. For each ratio, 10 mL of SWCNT dispersion was loaded into the multistage gel columns. Each gel column was packed with 1.4 mL of gel beads. The adsorbed nanotubes were eluted with 0.5 wt% DOC to compare the structural distribution of the adsorbed nanotubes.

As shown in Figure 5 and Figure S6 (Supporting Information), an increasing ratio of SC to SDS dramatically changed the structural distribution of the adsorbed nanotubes. Without the SC surfactant (Figure 5a), the adsorbed nanotubes in first column were mainly enriched with (6, 5) nanotubes, accompanied by some (6, 4), (7, 5), and (7, 6) nanotubes. However, by increasing the ratio of SC/SDS to 0.2 wt%/0.8 wt%, the content of the small-chiral-angle SWCNTs such as the (8, 3), (9, 1), and (9, 2) species increased in the adsorbed SWCNTs, while the contents of the (6, 4) and (6, 5) nanotubes decreased rapidly. Especially in the case of 0.5 wt% SDS + 0.5 wt% SC, the presence of higher contents of (7, 3), (8, 3), (9, 1), and (9, 2) nanotubes in the adsorbed SWCNTs were evident. These

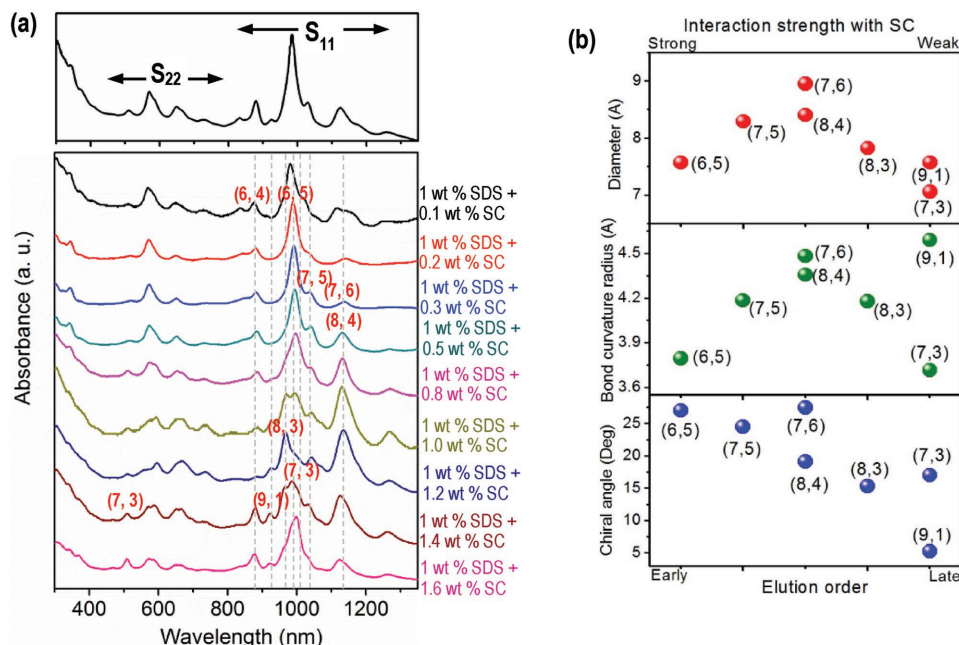


**Figure 4.** Optical analysis of the SWCNT fractions eluted with a stepwise increase in the SC concentration. a) Normalized optical absorption spectra. b) The elution order of distinct  $(n, m)$  species as a function of their diameters (top of panel), smallest bond curvature radius (middle of panel) and chiral angles (bottom of panel) at increasing the SC concentrations. In the lower panel of (a), the concentrations of SC are indicated on the right side of each spectrum.

results further confirm the preferential interaction of SC with SWCNTs having larger chiral angles,<sup>[32]</sup> and are different from the previous results.<sup>[21,22,30]</sup> Similar to the case of 1 wt% SDS, the small-diameter species exhibited a stronger adsorbability onto the gel due to their early adsorption in the columns (as shown in Figure 5c). However, when the ratio of SC to SDS increased to 0.8 wt%/0.2 wt%, the adsorption of SWCNTs was not observed, which implied that SC interacted more strongly with the SWCNTs than did SDS, and that a high ratio of SC to SDS led to a rapid decrease in their interaction with the gel.

### 2.3. The Synergistic Effect of Triple Surfactants in Amplifying the Interaction Difference between the SWCNTs and the Gel

Since the chiral structure of an SWCNT is solely determined by its diameter and chiral angle, the different selectivity of the surfactants SC, DOC, and SDS toward the chiral angles, diameters, and C–C bond curvatures of SWCNTs sufficiently suggested that the combination of these surfactants could synergistically enhance the structural recognition of the SWCNTs, which well explained the improved separation efficiency of SWCNTs by

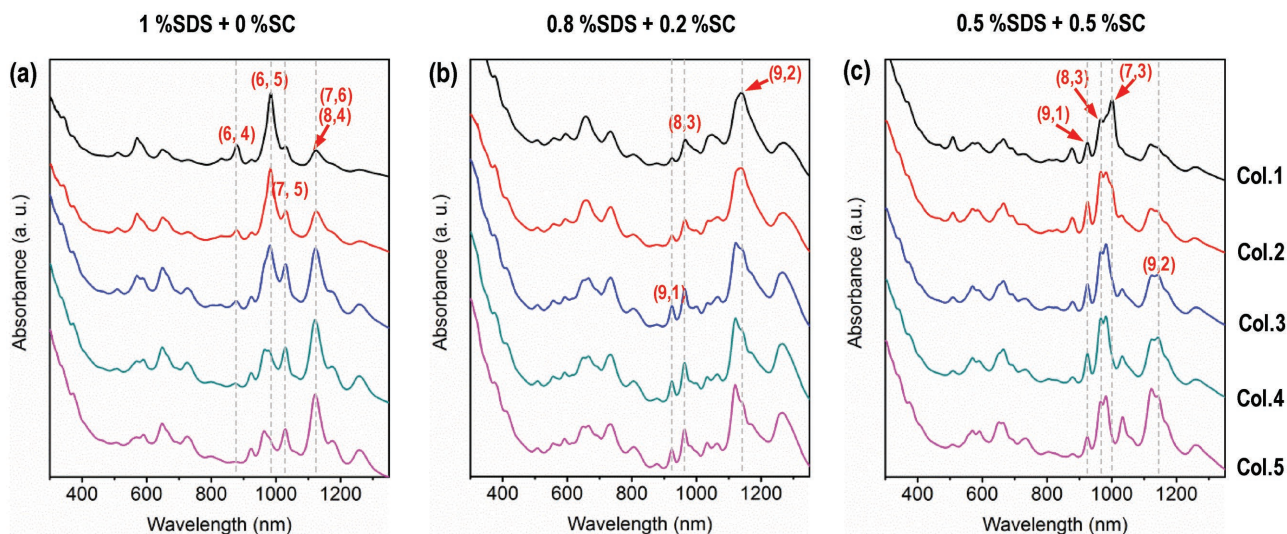


**Figure 5.** Normalized optical absorption spectra of the adsorbed nanotubes across different columns under different ratios of SC to SDS. a) 1.0 wt% SDS. b) 0.8 wt% SDS + 0.2 wt% SC. c) 0.5 wt% SDS + 0.5 wt% SC. Col. = Column.

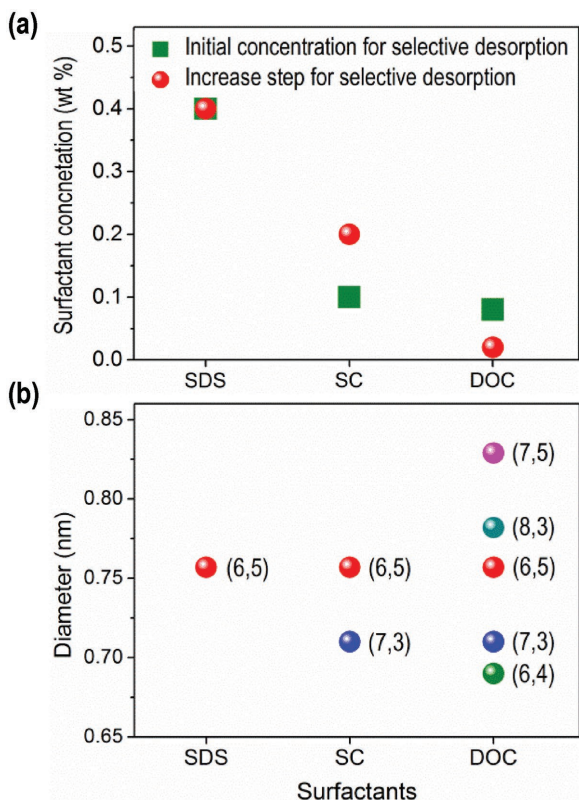


**Figure 6.** Analysis of the interaction between the various surfactants and the SWCNTs based on the results in Figures 2 and 4 and Figure S4 of the Supporting Information. a) Comparison of the initial concentrations and incremental steps of various surfactants for the selective desorption of SWCNTs and b) comparison of the distinct  $(n, m)$  single-chirality species separated via stepwise elution of different surfactants.

the use of cosurfactants in previous works.<sup>[19,21,32,34]</sup> The interaction strength of different surfactants with the SWCNTs is another important parameter for the separation of SWCNTs. A strong interaction between the surfactants and the SWCNTs would suppress the adsorption of SWCNTs onto the gel, thus exhibiting strong elution ability. The elution features of the three surfactants are summarized in **Figure 6**. The starting concentration and the increment step of SDS for the selective

desorption of SWCNTs was the largest at 0.4 wt%, while those of DOC were the smallest at 0.08 and 0.02 wt%, respectively. As shown in **Figure 6b**, five types of  $(n, m)$ -enriched species were separated by the stepwise elution process with DOC, while only (6, 5)-enriched species were separated by stepwise elution with SDS. The highest elution ability of DOC indicates its strongest interaction strength with the SWCNTs. By contrast, the lowest elution ability of SDS implies its weakest interaction with the SWCNTs. The interaction of SC with the SWCNTs and its structural identification ability are higher than that of SDS but lower than that of DOC. The structure of SC is very similar to that of DOC (**Figure 1b**). The lower interaction of SC with the SWCNTs possibly resulted from the hydrophilic hydroxyl groups in its molecule structure.

Because of their different interaction strengths with the SWCNTs, and thus the elution abilities, the surfactants DOC, SC, and SDS play different roles in the separation process of the SWCNTs. In order to separate the SWCNTs by gel chromatography, the selective adsorption of SWCNTs onto the gel is critical. The surfactant DOC is suitable for the selective desorption of SWCNTs because of its strong elution ability and identification ability for the SWCNTs. By contrast, SC and SDS are more suitable for dispersing the SWCNTs to enable their adsorption into the gel columns owing to their weaker interaction with the SWCNTs and lower elution ability. Therefore, the adsorbability of the SWCNTs dispersed by the cosurfactant system of SC and SDS in different ratios (namely, 1 wt% SDS + 0 wt% SC, 0.8 wt% SDS + 0.2 wt% SC, 0.5 wt% SDS + 0.5 wt% SC, and 0.2 wt% SDS + 0.8 wt% SC) was investigated. In these experiments, 0.2 mL of SWCNT dispersion was loaded into a gel column packed with 8 mL of gel beads (normal loading condition). The adsorbed nanotubes were eluted with 0.5 wt% DOC solution. As shown in **Figure 7**, at SC to SDS ratios lower than 0.5 wt%/0.5 wt%, the adsorbed nanotubes showed the same structural distribution as that of the semiconducting SWCNTs in the pristine HiPco-SWCNTs. However, in the case of 0.2 wt% SDS + 0.8 wt% SC, the loaded SWCNTs directly flowed through the gel column without adsorption. Thus, the surfactant system of 0.5 wt% SC + 0.5 wt% SDS provides the optimal condition that not only ensures the adsorption of SWCNTs onto the gel columns (**Figure 7**), but also effectively tunes the interaction difference between the various SWCNTs and the gel based on

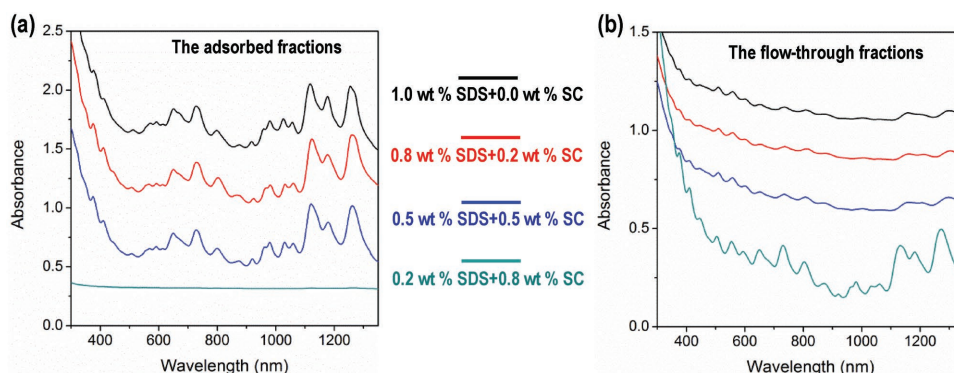


**Figure 7.** Optical absorption spectra of the adsorbed SWCNTs and flow-through fractions under different ratios of SC to SDS by the normal loading method. a) The adsorbed SWCNTs and b) the flow-through fractions. From top to bottom, the spectra correspond to the SDS to SC ratios of 1.0 wt% SDS + 0.0 wt% SC, 0.8 wt% SDS + 0.2 wt% SC, 0.5 wt% SDS + 0.5 wt% SC, and 0.2 wt% SDS + 0.8 wt% SC.

both the chiral angle and the diameter (Figures 2 and 4). This facilitates the selective desorption of the adsorbed SWCNTs by increasing the DOC concentration.

In the triple-surfactant system, the addition of SC can be performed by two approaches: First one, the SWCNTs were directly dispersed in the aqueous solution of 0.5 wt% SDS + 0.5 wt% SC and then overloaded into the gel columns (see Method 1 in Figure S7, Supporting Information). Second one, the SWCNTs were dispersed in an aqueous solution of 1 wt% SDS and overloaded into the gel columns (see Method 2 in Figure S8, Supporting Information). The SDS concentration in the gel column was changed to 0.5 wt% by eluting with an aqueous solution of 0.5 wt% SDS. The SC concentration was then in-situ tuned to 0.5 wt% by eluting the gel columns with 0.5 wt% SDS +  $x$  wt% SC, in which the SC concentration  $x$  was increased in small incremental steps, preventing the desorption of SWCNTs. Here, we performed parallel experiments to investigate the effect of the two methods on the separation of SWCNTs, which could give more insight into the interaction between the SWCNTs and the surfactants, and help to design new strategy to improve the separation efficiency of single-chirality SWCNTs. In both the methods, the selective desorption

of the adsorbed nanotubes was performed by the eluents 0.5 wt% SDS + 0.5 wt% SC +  $\gamma$  wt% DOC, in which the DOC concentration  $\gamma$  was incrementally increased from 0.019 to 0.085 wt% with an optimized incremental step of 0.002 wt% to 0.003 wt%. A larger incremental step would decrease the structural purities of the separated nanotubes (see Figure S9, Supporting Information). In the two methods, overloading was employed to narrow the structural distribution of the adsorbed SWCNTs, thus reducing the mutual disturbance of the different-structure species during the selective desorption. As shown in Figure S10 (Supporting Information), under normal loading conditions, the large-diameter SWCNTs with longer absorption wavelength were eluted together with the small-diameter SWCNTs without structural selectivity from the gel column, which dramatically reduced the purities of the separated SWCNTs.

The optical absorption spectra of the SWCNTs separated by the two methods are shown in Figure 8 and Figure S11, and Figures S12 and S13 (Supporting Information), respectively. The results achieved from the two methods were very similar. At each DOC concentration, single-chirality SWCNTs were desorbed from the gel columns, but their purities were slightly different. The optical absorption spectra of the highest-purity

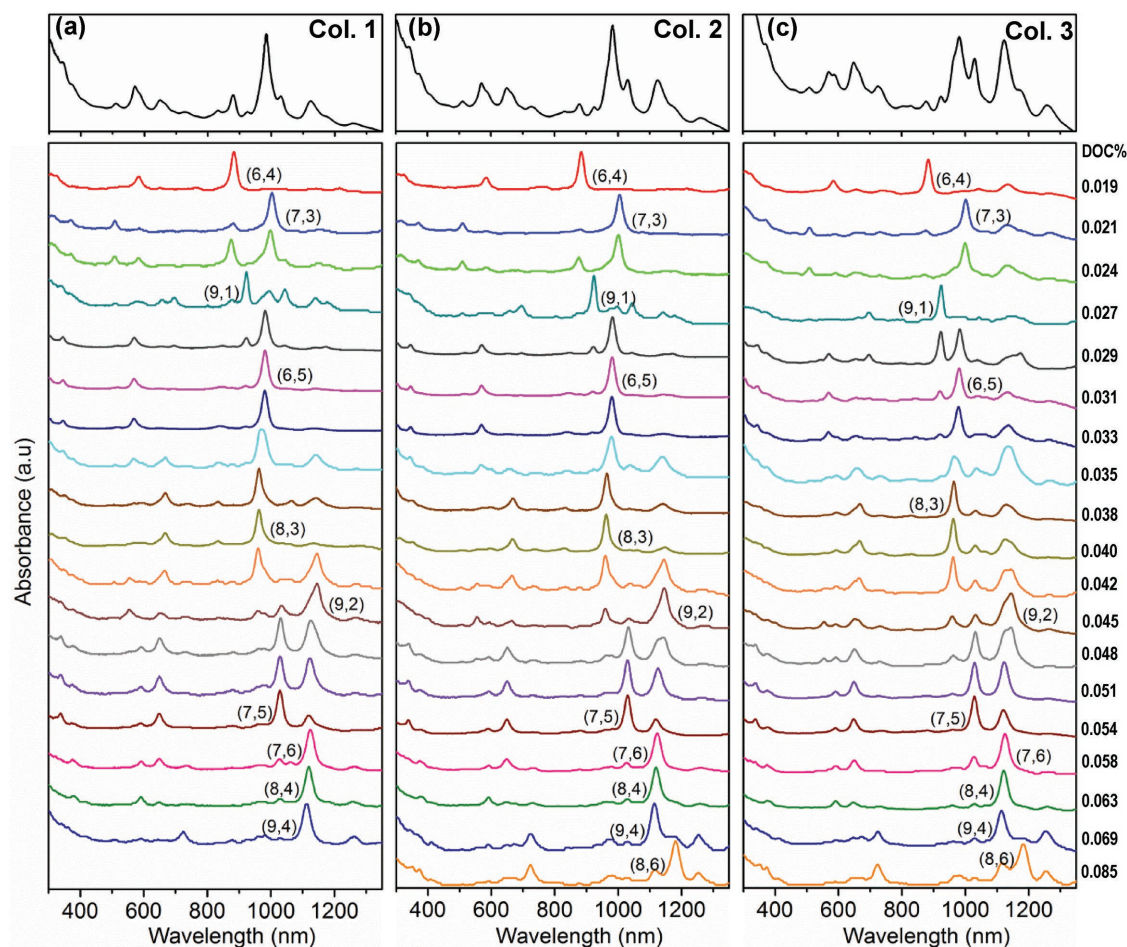


**Figure 8.** Normalized optical absorption spectra of the separated SWCNT fractions by a stepwise increase in the DOC concentration after in situ tuning of the interaction between the SWCNTs and the gel with SC (Method 2). a) Column 1, (b) Column 2, and (c) Column 3. In (a–c), the upper panels correspond to the adsorbed SWCNTs and the lower panels correspond to the eluted fractions. On the right, the concentrations of DOC are indicated.

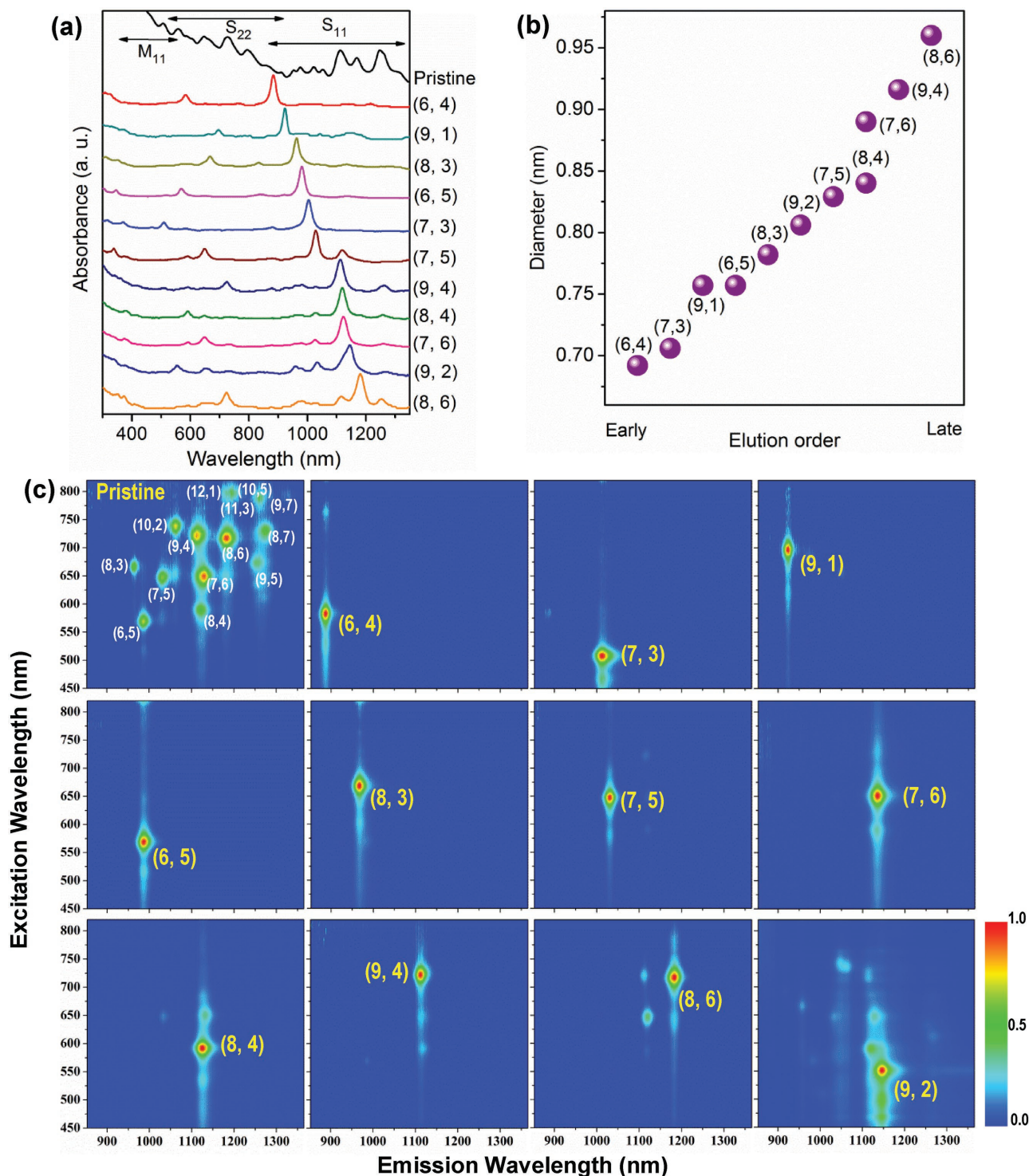


**Figure 9.** Optical characterization of the highest purity  $(n, m)$  species. a) Normalized optical absorption spectra, b) the relationship plot between the elution order and the diameters, and c) the photoluminescence map of the eluted single-chirality species shown in (a).

$(n, m)$  species are shown in **Figure 9a** and **Figure S14a** (Supporting Information). Eleven distinct near single-chirality  $(n, m)$  species were separated: (6, 4), (7, 3), (9, 1), (6, 5), (8, 3), (9, 2), (7, 5), (8, 4), (7, 6), (9, 4), and (8, 6). The purity evaluation of the separated  $(n, m)$  species was performed using a previously

described method.<sup>[24]</sup> The results were presented in **Figures S15** and **S16** of the Supporting Information. The purities of the separated  $(n, m)$  by the two methods were summarized in **Table S1** of the Supporting Information. It can be concluded that the purities of the (6, 5), (7, 5), (7, 6), (8, 6), and (9, 4)

nanotubes with larger-chiral angles separated by method 2 are clearly higher, possibly because of the difference in the  $(n, m)$  distribution of the SWCNTs adsorbed on the gel used for the following stepwise elution (Figure 5). As shown in Figure 9a and Figure S15 (Supporting Information), the purities of the  $(n, m)$  species separated by method 2 reached as high as 90% such as (6, 4), (6, 5), and (7, 3), which are much higher than that obtained from the SDS/DOC system (Figure 2a). More importantly, the types of the separated  $(n, m)$  species was more than twice of that obtained from the SDS/DOC system. The (9, 1), (9, 2), (8, 4), (7, 6), and (9, 4) SWCNTs species with small chiral angles could not be separated from the same adsorbed SWCNTs without the introduction of SC (Figure 2a), which indicated that the introduction of SC dramatically improved the separation efficiency of the SWCNTs. Besides, the presence of SC also prevented the mass desorption at the first elution step, despite the use of a high initial DOC concentration of 0.02 wt%, possibly because of their smaller difference in the affinity/or interaction with the SWCNTs. The separation of high-purity single-chirality  $(n, m)$  species was further confirmed by photoluminescence mapping (Figure 9c). As shown in Figure 9b and Figure S14b (Supporting Information), the relationship between the elution order  $(n, m)$  and their diameters displays a smooth elution tendency from small-diameter to large-diameter species, evidencing that the elution order was dominated by DOC because of its strong interaction with the SWCNTs. We speculate that the introduced DOC molecules possibly plugged into the SDS/SC surfactant coating and directly interacted with the nanotube surfaces, and thus forming a mixture-surfactant structure instead of a layered-surfactant structure. Additionally, the purities of the SWCNT fractions separated from the third column in the both methods were slightly lower than

those separated from columns 1 and 2 (Figure 8c; Figure S12c, Supporting Information). In the third column, more of the large-diameter SWCNTs were adsorbed. Possibly because the adsorbability of these large-diameter SWCNTs was weaker, the introduction of low-concentrations of DOC (extremely strong elution ability) easily induced nonselective desorption, similar to the case shown in Figure S10 of the Supporting Information. Therefore, for the separation of large-diameter SWCNTs, a different surfactant concentration ratio should be adopted.

As shown in Figure 8 and Figure S12 (Supporting Information), the same  $(n, m)$  species were desorbed at different DOC concentrations, indicating their different interaction with the gel, possibly due to enantiomeric separation.<sup>[19,26,40]</sup> The circular dichroism (CD) spectra of the separated fractions were recorded. As shown in Figure 10 and Figures S17 and S18 (Supporting Information), the CD spectra exhibited positive and negative CD peaks at the corresponding optical transition wavelengths,<sup>[19,26]</sup> evidencing the enantiomeric separation of the single-chiral (6, 4), (7, 3), (6, 5), (8, 3), and (7, 5) species. The relative purities of the various  $(n, m)$  enantiomer fractions were evaluated based on the background-corrected intensity of the CD and optical absorption at the  $E_{22}$  transition wavelength,<sup>[26]</sup> and the corresponding absorbance was acquired from their absorption spectra (Figures S17 and S18, Supporting Information). These results are presented in Table S2 (Supporting Information). The relative purities of the enantiomers (29.7–81.3 mdeg) are much higher than those of the enantiomers separated by a single surfactant (0.4–11.8 mdeg),<sup>[26]</sup> and those separated with other techniques.<sup>[16,17,19,41,42]</sup> Here, we ascribed the higher purities of the separated enantiomers to the selective interaction of the chiral surfactants SC and DOC with SWCNTs. High-purity enantiomers can be achieved by long-term dispersion and ultracentrifugation of the SWCNT dispersions to

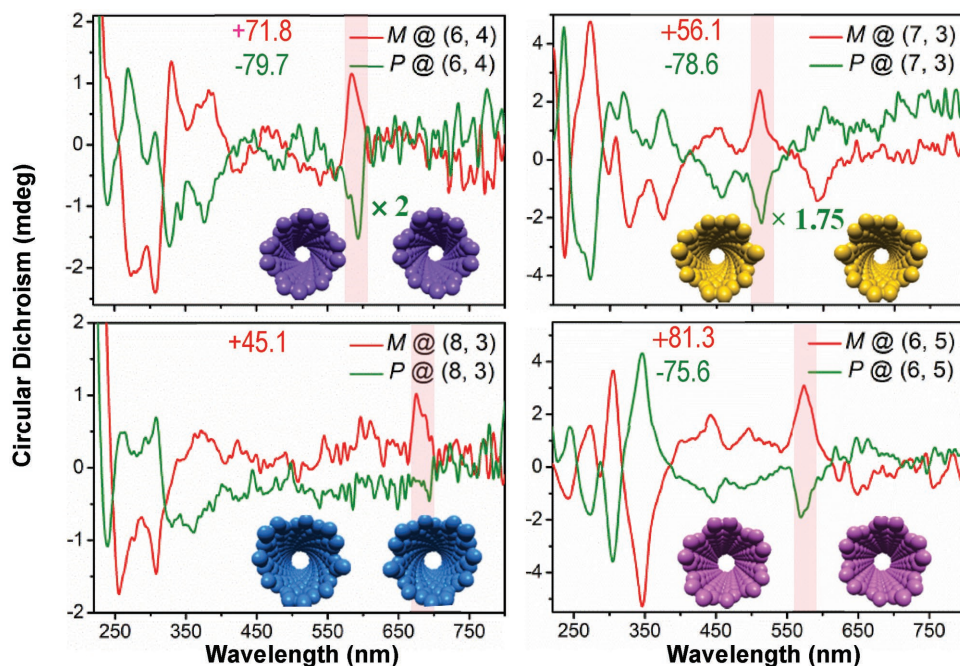


**Figure 10.** Typical circular dichroism (CD) spectra of the eluted single-chirality species. The relative purities of the separated enantiomers are indicated in each panel. The relative purity for the right-handed enantiomer (8, 3) is unavailable because the CD intensity at  $E_{22}$  was difficult to evaluate. The complete CD and optical absorption spectra of the separated enantiomers are presented in Figures S17 and S18 (Supporting Information).

remove the nanotubes bundles and by multistep separation at the expense of the raw materials and separation efficiency.<sup>[34]</sup>

### 3. Conclusions

The selective interaction of the surfactants DOC, SC, and SDS with the SWCNTs were systematically investigated by gel chromatography to experimentally demonstrate the selective interaction of different surfactants with SWCNT structures. DOC preferentially interacted with small-diameter SWCNTs and exhibited stronger interaction strength and higher structure recognition ability. SC selectively interacted with large-chiral-angle SWCNTs, and showed interaction strength stronger than that of SDS but weaker than that of DOC. Combining with the proved selectivity of SDS molecules in the interaction with SWCNTs having small C–C bond curvatures, we clarified that the synergistic effect of the cosurfactants enlarged the interaction difference between the different ( $n$ ,  $m$ ) SWCNTs and the gel and thus dramatically improved the separation efficiency and purities, simultaneously achieving the separation of distinct ( $n$ ,  $m$ ) single-chirality species and their enantiomers. The present results provide a more comprehensive understanding of the structural separation of SWCNTs by the surfactant sorting methods, which could help to further improve the separation efficiency and purities of single-structure SWCNTs, thus accelerating their technical applications in optoelectronic, bio-medicine and new functional materials.

### 4. Experiment Section

**Dispersion and Purification of SWCNTs:** HiPco-SWCNTs (R1-794,  $1.0 \pm 0.3$  nm in diameter, Nanointegris) were dispersed in 1 wt% SDS (99%, Sigma-Aldrich) aqueous solution (15 mg SWCNT/15 mL SDS solution) using an ultrasonic probe homogenizer (Sonifire 450D, Branson) for 1.5 h at 30 W. During sonication, the bottle containing the sample solution was immersed in a water bath at 15 °C to prevent heating. The resulting sample was then centrifuged at  $210\,000 \times g$  for 30 min using an ultracentrifuge (S50A, Hitachi CS150FNX) to remove bundles and impurities. Approximately 80% of the supernatant was recovered and used as the parent SWCNT dispersion.

**Detecting the Selective Interaction between the Surfactants and the SWCNTs:** The selective interaction between the surfactants and the SWCNTs was detected by a stepwise elution process. Specifically, 10 mL of SWCNT dispersion was applied to a column packed with 1.4 mL of gel beads (Sephacryl S-200 HR, GE Healthcare, lot 10102247), and the unadsorbed nanotubes were washed by 1 wt% SDS solution. The SWCNTs in the gel column were desorbed by the eluent 1 wt% SDS +  $x$  wt% A, where A represents one of the surfactants SDS, SC, or DOC and  $x$  denotes the concentration of the corresponding surfactant A. During the stepwise elution, the concentration  $x$  was increased with a step of 0.4 wt% for SDS (99%, Sigma-Aldrich), 0.02 wt% for DOC (97%, Sigma-Aldrich), and 0.1–0.2 wt% for SC (99%, Sigma-Aldrich), until no additional SWCNTs could be eluted from the gel columns. The SWCNTs eluted at each step were fractionally collected with 1.5 mL of 1 wt% SDS +  $x$  wt% A and used for optical measurements. The schematic diagram of this process is presented in Figure S1 of the Supporting Information. Before the experiments, the gel columns were prepared by loading 1.4 mL of allyl dextran-based gel beads (Sephacryl S-200 HR, GE Healthcare) into a 10 mL medical syringe (inner diameter = 1.6 cm).

**Synergistically Tuning the Interaction between the SWCNTs and the Gel with Triple Surfactants:** Two methods were adopted to synergistically tune

the interaction between the SWCNTs and the gel with triple surfactants. In the first method, HiPco-SWCNTs were dispersed directly in a mixture of 0.5 wt% SDS + 0.5 wt% SC solution. 10 mL of SWCNT dispersion was applied to a column packed with 1.4 mL of gel in the surfactant environment of 0.5 wt% SDS + 0.5 wt% SC (overloading case). After the unadsorbed nanotubes were completely washed away, the nanotubes adsorbed onto the gel were eluted stepwise by a series of eluents, where the concentrations of SDS and SC were respectively fixed at 0.5 wt%, while the content of DOC was increased until no desorption could be detected. The eluted nanotubes were also collected fractionally with 1.5 mL of 0.5 wt% SDS + 0.5 wt% SC +  $x$  wt% DOC. The corresponding schematic diagram is given in Figure S7 of the Supporting Information. For comparison, the effect of normal loading on the selective desorption of the SWCNTs from gel was also investigated, in which 0.2 mL of SWCNT dispersion was loaded into a gel column packed with 8 mL of gel beads.

The difference in the second method is that the selective adsorption of the surfactant SC onto the SWCNTs was performed in the gel columns. Specifically, 10 mL of SWCNT/1 wt% SDS dispersion was loaded into a gel column packed with 1.4 mL of gel beads followed by washing away of the unadsorbed SWCNTs using 1 wt% SDS. Next, the surfactant environment was changed to 0.5 wt% SDS by eluting the gel column with 0.5 wt% SDS. The surfactant environment was then altered to 0.5 wt% SDS + 0.5 wt% SC by stepwise elution of the column with a series of eluents containing 1 wt% SDS +  $x$  wt% SC in which the SC concentration  $x$  was incrementally increased from 0 to 0.5 wt% with a small step. Finally, the nanotubes were selectively desorbed from the gel in the same way as mentioned in method 1. The corresponding schematic diagram for this experiment is presented in Figure S8 of the Supporting Information.

**Optical Measurements:** The optical absorption spectra were recorded by using a UV–vis–NIR spectrophotometer (UV-3600, Shimadzu) in the wavelength range of 200–1350 nm. Photoluminescence contour maps were measured using a spectrofluorometer (Nanolog, Horiba) equipped with a liquid nitrogen-cooled InGaAs detector. CD spectra were recorded using a CD spectrometer (J-1500, JASCO) in the wavelength range of 200–900 nm. For each of the measured samples, a corrected spectrum was obtained by subtracting a reference CD spectrum recorded under the same conditions with an aqueous solution of the cosurfactant system.

### Supporting Information

Supporting Information is available from the Wiley Online Library or from the author.

### Acknowledgements

This work was supported by the National Natural Science Foundation of China (Grant Nos. 51472264, 11634014, and 51361022), and the Key Research Program of Frontier Sciences, CAS, Grant No. QYZDB-S5W-SYS028. H.P.L. thanks support by the Recruitment Program of Global Youth Experts and the “100 talents project” of CAS.

### Conflict of Interest

The authors declare no conflict of interest.

### Keywords

carbon nanotubes, gel chromatography, interaction detecting, structural separation, surfactants

Received: June 21, 2017

Revised: October 2, 2017

Published online:

- [1] J. W. G. Wilder, L. C. Venema, A. G. Rinzler, R. E. Smalley, C. Dekker, *Nature* **1998**, 391, 59.
- [2] P. Avouris, Z. Chen, V. C. Perebeinos, *Nat. Nanotechnol.* **2007**, 2, 605.
- [3] G. S. Tulevski, A. D. Franklin, D. Frank, J. M. Lobe, Q. Cao, H. Park, A. Afzali, S. Han, J. B. Hannon, W. Haensch, *ACS Nano* **2014**, 8, 8730.
- [4] M. S. Purewal, B. H. Hong, A. Ravi, B. Chandra, J. Hone, P. Kim, *Phys. Rev. Lett.* **2007**, 98, 186808.
- [5] M. Engel, J. P. Small, M. Steiner, M. Freitag, A. A. Green, M. C. Hersam, *ACS Nano* **2008**, 2, 2445.
- [6] A. D. Franklin, M. Luisier, S. J. Han, G. Tulevski, C. M. Breslin, L. Gignac, M. S. Lundstrom, W. Haensch, *Nano Lett.* **2012**, 12, 758.
- [7] M. M. Shulaker, G. Hills, N. Patil, H. Wei, H. Chen, H. S. Wong, S. Mitra, *Nature* **2013**, 507, 526.
- [8] L. Yang, S. Wang, Q. Zeng, Z. Zhang, T. Pei, Y. Li, L. Peng, *Nat. Photonics* **2011**, 5, 672.
- [9] R. M. Jain, R. Howden, K. Tvrđy, S. Shimizu, A. J. Hilmer, T. P. McNicholas, K. K. Gleason, M. S. Strano, *Adv. Mater.* **2012**, 24, 4436.
- [10] W. H. Chiang, R. M. Sankaran, *Nat. Mater.* **2009**, 8, 882.
- [11] F. Yang, X. Wang, D. Zhang, J. Yang, D. Luo, Z. Xu, J. Wei, J. Q. Wang, Z. Xu, F. Peng, X. Li, R. Li, Y. Li, M. Li, X. Bai, F. Ding, Y. Li, *Nature* **2014**, 510, 522.
- [12] J. R. Sanchez-Valencia, T. Dienel, O. Groning, I. Shorubalko, A. Mueller, M. Jansen, K. Amsharov, P. Ruffieux, R. Fasel, *Nature* **2014**, 512, 61.
- [13] S. Zhang, L. Kang, X. Wang, L. Tong, L. Yang, Z. Wang, K. Qi, S. Deng, Q. Li, X. Bai, F. Ding, J. Zhang, *Nature* **2017**, 543, 234.
- [14] M. Zheng, A. Jagota, E. D. Semke, B. A. Diner, R. S. Mclean, S. R. Lustig, R. E. Richardson, N. G. Tassi, *Nat. Mater.* **2003**, 2, 338.
- [15] X. Tu, S. Manohar, A. Jagota, M. Zheng, *Nature* **2009**, 460, 250.
- [16] F. Wang, K. Matsuda, A. F. Rahman, X. Peng, T. Kimura, N. Komatsu, *J. Am. Chem. Soc.* **2010**, 132, 10876.
- [17] K. Akazaki, F. Tshimitsu, H. Ozawa, T. Fujigaya, N. Nakashima, *J. Am. Chem. Soc.* **2012**, 134, 12700.
- [18] M. S. Arnold, A. A. Green, J. F. Hulvat, S. I. Stupp, M. C. Hersam, *Nat. Nanotechnol.* **2006**, 1, 60.
- [19] S. Ghosh, S. M. Bachilo, R. B. Weisman, *Nat. Nanotechnol.* **2010**, 5, 443.
- [20] C. Y. Khripin, J. A. Fagan, M. Zheng, *J. Am. Chem. Soc.* **2013**, 135, 6822.
- [21] J. A. Fagan, C. Y. Khripin, C. A. Silvera Batista, J. R. Simpson, E. H. Háróz, A. R. Hight Walker, M. Zheng, *Adv. Mater.* **2014**, 26, 2800.
- [22] N. K. Subbaiyan, S. Cambré, A. N. Parra-Vasquez, E. H. Háróz, S. K. Doorn, J. G. Duque, *ACS Nano* **2014**, 8, 1619.
- [23] T. Tanaka, Y. Urabe, D. Ishide, H. Kataura, *Appl. Phys. Express* **2009**, 2, 125002.
- [24] H. Liu, D. Nishide, T. Tanaka, H. Kataura, *Nat. Commun.* **2011**, 2, 309.
- [25] H. Liu, T. Tanaka, Y. Urabe, H. Kataura, *Nano Lett.* **2013**, 13, 1996.
- [26] H. Liu, T. Tanaka, H. Kataura, *Nano Lett.* **2014**, 14, 6237.
- [27] P. Zhao, E. Einarsson, R. Xiang, Y. Murakami, S. Maruyama, *J. Phys. Chem. C* **2010**, 114, 4831.
- [28] P. Zhao, E. Einarsson, G. Lagoudas, J. Shiomi, S. Chiashi, S. Maruyama, *Nano Res.* **2011**, 4, 623.
- [29] T. A. Shastry, A. J. Morriscohen, E. A. Weiss, M. C. Hersam, *J. Am. Chem. Soc.* **2013**, 135, 6750.
- [30] R. M. Jain, M. Bennaïm, M. P. Landry, M. S. Strano, *J. Phys. Chem. C* **2015**, 119, 22737.
- [31] A. Hirano, T. Tanaka, Y. Urabe, H. Kataura, *ACS Nano* **2013**, 7, 10285.
- [32] Y. Yomogida, T. Tanaka, M. Zhang, M. Yudasaka, X. Wei, H. Kataura, *Nat. Commun.* **2016**, 7, 12056.
- [33] X. Zeng, J. Hu, X. Zhang, N. Zhou, W. Zhou, H. Liu, S. Xie, *Nanoscale* **2015**, 7, 16273.
- [34] X. Wei, T. Tanaka, Y. Yomogida, N. Satio, R. Saito, H. Kataura, *Nat. Commun.* **2016**, 7, 12899.
- [35] T. Tanaka, Y. Urabe, D. Nishide, H. Kataura, *J. Am. Chem. Soc.* **2011**, 133, 17610.
- [36] R. B. Weisman, S. M. Bachilo, *Nano Lett.* **2003**, 3, 1235.
- [37] H. Liu, Y. Feng, T. Tanaka, Y. Urabe, H. Kataura, *J. Phys. Chem. C* **2010**, 114, 9270.
- [38] W. Wenseleers, I. I. Vlasov, E. Goovaerts, E. Obraztsova, A. S. Lobach, A. Bouwen, *Adv. Funct. Mater.* **2004**, 14, 1105.
- [39] N. R. Tummala, A. Striolo, *ACS Nano* **2009**, 3, 595.
- [40] T. Tanaka, Y. Urabe, T. Hirakawa, H. Kataura, *Anal. Chem.* **2015**, 87, 9467.
- [41] M. Zhang, C. Y. Khripin, J. A. Fagan, P. McPhie, Y. Ito, M. Zheng, *Anal. Chem.* **2014**, 86, 3980.
- [42] A. A. Green, M. C. Duch, M. C. Hersam, *Nano Res.* **2009**, 2, 69.